14th World Congress in Computational Mechanics (WCCM)
ECCOMAS Congress 2020
Virtual Congress: 11 – 15 January 2021
F. Chinesta, R. Abgrall, O. Allix and M. Kaliske (Eds)

NON-PRISMATIC BEAMLIKE STRUCTURES WITH 3D CROSS-SECTIONAL WARPING

G. MIGLIACCIO[1]

[1]Department of Civil and Industrial Engineering, University of Pisa
Largo Lucio Lazzarino 2, 56122, Pisa, Italy
giovanni.migliaccio.it@gmail.com

Key words: tapered beams, cross-sectional warping, large displacements.

Abstract. Many complex engineering structures, e.g. blades of wind turbines and helicopters, are beamlike and non-prismatic. They may be tapered, twisted and curved in their unstressed state, undergo large displacements of the centre-line, and cross-sectional warping in and out of plane. For their structural modeling, an approach based on beam elements can be the best compromise between computational efficiency and accuracy, but classical beam models (see, for example, the monumental Love's treatise) may not be sufficient. Better results may be obtained by exploiting geometrically exact and asymptotic approaches. This paper proposes a physical-mathematical model for the aforementioned non-prismatic structures. Analytical results obtained for small warping and strain fields are presented and compared to the results obtainable from nonlinear 3D-FEM analyses.

1 INTRODUCTION

Beamlike structures, e.g. helicopter blades, wind blades, components of civil buildings and bridges, are widespread in engineering applications. Such structures may be tapered, twisted, and even curved in their unstressed state, have fully deformable transverse cross-sections, and undergo large displacements. For their structural modelling the best compromise between computational efficiency and accuracy can be obtained via schematizations based on suitable beam elements [1-3]. However, classical beam models for extension, twisting, bending and shear deformation, e.g. [4-6], may not be sufficient. Models based on geometrically exact and asymptotic approaches can provide better results [7]. Over the years several models have been proposed for beamlike bodies [8-13], and most of them are also summarized in reviews (e.g. [14-16]). Nevertheless, non-prismatic cases still require investigation. Generally speaking, the geometry of the non-prismatic beamlike body must be appropriately described, as the taper, twist, and curvature are important geometric features and should be explicitly included in the model. Moreover, the analysis should not be restricted to small displacements. The model should provide the stress and strain fields in the three-dimensional body, be rigorous and application-oriented, and provide classical results for prismatic cases. Following such main guidelines, a physical-mathematical model for the aforementioned structures is proposed in this work. Specifically, this paper addresses the mechanical modelling of non-prismatic beamlike elements subjected to large displacements of the centre-line's points, cross-sectional

warping in and out of plane, and small strain, with particular focus on the effects of important geometric features, such as the cross-sectional taper. A model suitable for the problem at hand is introduced in section 2. Analytical results obtained by its application are presented in section 3. Numerical examples and comparisons with the results from nonlinear 3D-FEM simulations are finally shown in section 4.

2 MECHANICAL MODEL

An important point in modeling structures subject to large displacements is the description of their motion [17-22]. We describe a beamlike structure as a collection of deformable plane figures (transverse cross-sections) along a 3D curve (beam's centre-line). The displacement from the reference to the current state of each cross-sectional point consists of a global rigid motion onto which a local warping motion is superposed. In this way, the cross-sectional local motion can be examined independently of the global motion, and it is possible to consider the global motion to be large, while the local warping motion and the strain may be small.

2.1 Kinematics and strain measures

We begin introducing two local triads of orthogonal unit vectors. The first is the reference local triad, b_i, with b_1 tangent to the reference centre-line. It is a function of the reference arc-length s, i.e. $b_i=b_i(s)$. The second triad, a_i, is an image of b_i in the current state. It depends on the arc-length s and time t, i.e. $a_i=a_i(s,t)$. In general, the orientation of a_i and b_i relative to a fixed rectangular frame, c_i, can be defined as

$$a_i = Ac_i, \quad b_i = Bc_i \tag{1}$$

where A and B are proper orthogonal tensor fields. Figure 1 schematizes the reference and current states of the structure in terms of centre-lines and cross-sections. A cross-section in the reference state is contained in the plane of b_2 and b_3. In the current state it may not remain plane (i.e. un-warped) and may not belong to the plane of a_2 and a_3. Its possibly warped state is in fact attained by superposing the aforementioned warping motion to the position of the points of the un-warped cross-section (as shown in Figure 1, right).

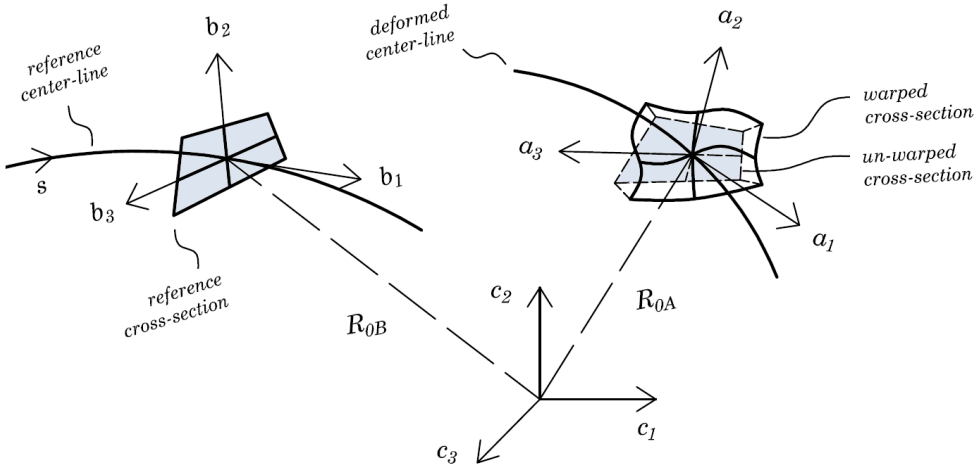

Figure 1: Schematic of reference and current states in terms of centre-lines, cross-sections and local frames

Two mapping functions, R_A and R_B, identify the positions of the structure's points in the current and reference states, respectively. The reference mapping function is

$$R_B(z_i) = R_{0B}(z_1) + x_\alpha(z_i) b_\alpha(z_1) \tag{2}$$

where R_{0B} provides the position of the reference centre-line relative to triad c_i, b_α are vectors of the reference local triad in the plane of the reference cross-section, x_α identify the position of such cross-section's points relative to the reference centre-line, and z_i are three independent mathematical variables which do not depend on time. More precisely, z_1 is equal to the reference arc-length s, while z_α belong to a bi-dimensional domain which is used to map the positions, x_α, of the cross-sections points.

Throughout this paper, Greek indices take values 2 and 3, Latin indices assume values 1, 2 and 3, and repeated indices are summed over their range.

It is worth noting that x_k may or may not be equal to z_k, depending on the modeling approach adopted and the structure to be modeled. Here we choose relations between x_k and z_k to explicitly model the shape of the non-prismatic beams considered in this work. In particular, the spanwise variation of the cross-sectional shapes is modeled via the map

$$x_i = \Lambda_{ij} z_j \tag{3}$$

where Λ_{ij} are functions of z_1. We consider curved and twisted beamlike bodies with bi-tapered transverse cross-sections, with map (3) reducing to

$$x_1 = z_1, \quad x_2 = z_2 \Lambda_2(z_1), \quad x_3 = z_3 \Lambda_3(z_1) \tag{4}$$

where coefficients Λ_α are functions of z_1.

A suitable choice of such functions enables reproducing several interesting shapes. Figure 2, for example, shows a beamlike structure with a three-dimensional curved centre-line, while the transverse cross-sections have dimensions and orientations which change from the root to the tip of the structure, that is, they are bi-tapered and pre-twisted.

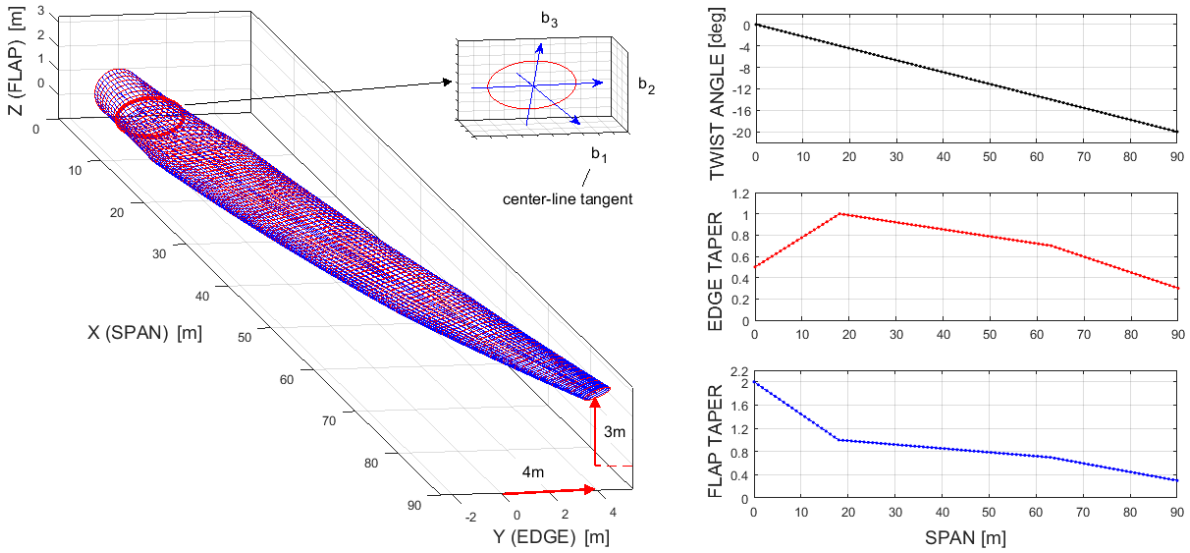

Figure 2: Example non-prismatic beamlike structure (left), and its twist and taper parameters (right)

The position of the structure's points in the current state are defined in a similar manner by the (current) mapping function

$$R_A(z_i,t) = R_{0A}(z_1,t) + x_\alpha(z_i)a_\alpha(z_1,t) + w_k(z_i,t)a_k(z_1,t) \tag{5}$$

where R_{0A} provides the positions of the centre-line's points in the current state, while w_k are the components of the 3D warping displacement with respect to a_k, introduced to describe the structure's deformed state without a-priori approximations.

We now introduce the kinematical variables we use to describe the motion of the structure, starting with the orthogonal tensor field T, which provides the relative orientation between a_i and b_i, and the skew tensor fields K_A and K_B, defined as follows

$$T = AB^T, \quad K_A = A'A^T, \quad K_B = B'B^T \tag{6}$$

The apex prime denotes the derivative with respect to the arc-length s. By combining equations (6), the following identity holds

$$T^T T' = T^T K_A T - K_B \tag{7}$$

The left side of (7) defines a skew tensor field, hereafter denoted as K. The corresponding axial vector, k, can be determined by the relation

$$k = T^T k_A - k_B \tag{8}$$

where the vector fields k_A and k_B are axial vectors of the skew tensors K_A and K_B. Those vectors are referred to here as curvature vectors. In particular, k turns out to be the difference between the back-rotated current curvature k_A and the reference curvature k_B. Therefore, k contains information on the curvature change between the current and reference states.

Similarly, the vector field γ, which is associated to the difference between the current and reference centre-line tangent vectors, is defined as follows

$$\gamma = T^T R'_{0A} - R'_{0B} \tag{9}$$

We also introduce the skew tensor field Ω, whose axial vector is called ω, which is related to the variation in the current local triad a_i over the time t, as follows

$$\Omega = \dot{A}A^T \tag{10}$$

The apex dot denotes the derivative over time t. The local triad b_i does not depend on time and so does function R_{0B}. On the contrary, R_{0A} can change over time. Its variation is the time rate of change in the position of the current centre-line's points, v_0, that is

$$\dot{R}_{0A} = v_0 \tag{11}$$

By exploiting (6)-(11), we can also write kinematic relations which provide the time rate of vector fields γ and k as functions of vector fields v_0 and ω, as follows

$$\begin{aligned} v_0' - \omega \wedge R'_{0A} &= T\dot{\gamma} \\ \omega' &= T\dot{k} \end{aligned} \tag{12}$$

where the operator ∧ is the usual cross-product.

Hereafter γ and k are also referred to as 1D strain measures, while the Green-Lagrange strain tensor E is referred to as 3D strain measure. Such tensor is moreover written in a form based on the assumptions of small warping and strain fields considered in this work. In particular, we assume that the reference dimension, *h*, of the cross-sections is much smaller that the characteristic length, *L*, of the centre-line (the beam is slender); the beam's curvatures are much smaller than *1/h*; the warping fields, w_k, are considered small in the sense that their maximum order of magnitude is $h\varepsilon$, $\varepsilon<<1$ being a non-dimensional parameter, while the order of their derivative with respect to z_1 is at most $\varepsilon h/L$. In general, all components of the 1D and 3D strain measures are assumed to be small in the sense that their order of magnitude is at most ε. For the considered structure, the strain tensor E can be written in the form

$$E \simeq \frac{T^T H + H^T T}{2} - I \tag{13}$$

where tensor H, which is the gradient of the current position R_A with respect to the reference position R_B, is defined as follows

$$H = \frac{\partial R_A}{\partial R_B} \tag{14}$$

2.2 Stress measures and constitutive model

Given the strain tensor E, the corresponding stress fields in the structure can be determined when a constitutive model is chosen. Limiting our attention to elastic bodies in a purely mechanical theory, in the case of small strain, the second (symmetric) Piola-Kirchhoff stress tensor, S, is expressed in terms of the Green-Lagrange strain tensor, E, as follows

$$S = 2\mu\, E + \lambda tr E\, I \tag{15}$$

where μ and λ are known material parameters and I is the identity tensor [23].

We can now define the stress resultants on each transverse cross-section of the structure, in terms of force and moment resultants, F and M, as follows

$$\begin{aligned} F &= \int_\Sigma P_{i1} a_i \\ M &= \int_\Sigma x_\alpha P_{i1}\, a_\alpha \wedge a_i \end{aligned} \tag{16}$$

In (16), Σ is the domain corresponding to the cross-section on which integration is performed, the force and moment vector fields, F and M, depend on arc-length s, and the components P_{ij} of the first Piola-Kirchhoff stress tensor, P, are defined as follows

$$P_{ij} = P \cdot a_i \otimes b_j \tag{17}$$

where symbol · is the usual scalar (or dot) product, symbol ⊗ is the usual tensor (or dyadic) product and, in the considered case, P=TS. In the present case it is moreover possible to write the classical Cauchy stress tensor, C, as $C=TST^T$.

2.3 Expended power and balance equations

To complete the model formulation, we introduce the principle of expended power and the balance equations for the considered structure. First of all, we assume that the beamlike body studied in this paper is three-dimensional and hyper-elastic [23]. Its interactions with the external environment are quantified, for each velocity field attainable by the body, through the following linear functional of its velocity field, Π_e, called the external power

$$\Pi_e = \int_{\partial V} p \cdot v + \int_V b \cdot v \tag{18}$$

In (18), b are body loads per unit reference volume V, p are surface loads per unit area of the reference boundary ∂V, and v is the referential description of the time rate of the current position of the body's points, given by

$$v = v_0 + \omega \wedge x_\alpha b_\alpha + w^{\bullet} \tag{19}$$

where $w^{\bullet}$ is the time rate of the warping displacement.

Interactions among different parts of the body are instead quantified by the internal power Π_i, which is defined as follows

$$\Pi_i = \frac{d}{dt}\int_V \Phi \tag{20}$$

where Φ is the energy density of the body, defined as twice the scalar product of tensor fields S and E (i.e. $2\Phi = S \cdot E$).

According to the principle of expended power, for any velocity field attainable by the body, its interactions with the external environment and among its parts are such that at any value of the evolution parameter t the total power vanishes (i.e. $\Pi_e = \Pi_i$). Exploitation of such principle is a usual technique in continuum mechanics to obtain balance equations in terms of the unknowns of the problem (see, e.g., [13] and [23]). In our case, it makes it possible to write balance equations for the stress resultants, F and M, in the form

$$\begin{aligned} F' + F_s &= 0 \\ M' + R'_{0A} \wedge F + M_s &= 0 \end{aligned} \tag{21}$$

where F_s and M_s are the resultants of the body and surface external loads per unit length of the reference centre-line. The same principle also enables writing balance equations to determine the warping fields, w_k, which govern the cross-sectional deformation. In particular, in the case in which the body loads and surface actions on the beam's lateral surface are neglected in calculating the warping fields, or vanish, it is possible to reduce the determination of the warping fields, w_k, to those that verify the following variational statement

$$\delta \int_V \Phi = 0 \tag{22}$$

where the symbol δ denotes the variation of the energy function with respect to the warping fields. Note that suitable warping fields satisfying (22) can be obtained via the corresponding Euler-Lagrange equations [24] by using numerical methods or, in particular cases, by means of analytical approaches providing closed-form results, as is discussed in the following.

2.4 Cross-sectional warping and centre-line deflection

So far we have introduced the main ingredients of our modeling approach for the structures considered in this work, which are three-dimensional, beamlike, slender, and non-prismatic, and have defined the strain measures, stress measures, and balance equations we use to describe their mechanical behavior. By exploiting such ingredients, the resolution of the three-dimensional nonlinear elasticity problem for the aforementioned structures is now reduced to the solution of two main problems: the first governs the cross-sectional warping motion and its strong formulation can be given in terms of partial differential equations (PDEs) defined over a reference bi-dimensional domain (as is further discussed in the following section). The second problem governs the centre-line motion and can be expressed in terms of a set of nonlinear ordinary differential equations (ODEs) defined over a reference line (as in [18], for instance).

Specifically, in the following we exploit condition (22) to obtain the PDEs problem the solution of which enables determining the warping of the transverse cross-sections (and show a case in which we can obtain analytical closed-form solutions). The displacements of the centre-line's points are instead determined by solving the nonlinear ODEs problem based on the balance equations (21) for the stress resultants and the corresponding kinematic and constitutive relations introduced in the previous sections 2.1-2.3. Such nonlinear problem is integrated (numerically) with respect to arc-length s.

3 ANALYTICAL RESULTS

The stress and strain fields in the considered structure are determined by exploiting condition (22). To this end, we use the corresponding Euler-Lagrange equations, in which we keep the terms up to the order $\varepsilon h/L$. In this way we obtain a mathematical problem based on partial differential equations (PDEs) with Neumann-type boundary conditions the solution of which enables determining the components of E. In doing this, we choose the current local triads to be tangent to the current centre-line, while possible shear deformations are directly accounted for through the warping fields. Note that hereafter we focus only on the effects of the cross-sectional taper on the stress and strain fields; other geometric effects, such those related to the cross-sectional pre-twist, are not considered.

Proceeding in this way, the components E_{11}, E_{21} and E_{31} of tensor E, associated to the out-of-plane deformation of the transverse cross-sections, can be written in the form

$$\begin{aligned} E_{11} &= k_2 x_3 - k_3 x_2 + \gamma_1 + e_{1,1} \\ 2E_{21} &= e_{1,2} - k_1 x_3 + 2(1+\nu)(k_2 x_3 - k_3 x_2 + \gamma_1)\Lambda_2^{-1}\Lambda_2' x_2 + e_2 \\ 2E_{31} &= e_{1,3} + k_1 x_2 + 2(1+\nu)(k_2 x_3 - k_3 x_2 + \gamma_1)\Lambda_3^{-1}\Lambda_3' x_3 + e_3 \end{aligned} \tag{23}$$

where $E_{ij} = E \cdot b_i \otimes b_j$, υ is Poisson's ratio, the subscript comma denotes the derivative with respect to x_i, and the scalar fields e_1, e_2, e_3 can be obtained by solving the PDEs problems

$$\begin{aligned} & e_{1,22} + e_{1,33} = 0 \quad in\ \Sigma \\ & (e_{1,2} - k_1 x_3) n_2 + (e_{1,3} + k_1 x_2) n_3 = 0 \quad on\ \partial\Sigma \end{aligned} \tag{24}$$

$$
\begin{aligned}
&e_{2,2}+e_{3,3}=a_2x_2+a_3x_3 \quad in\ \Sigma\\
&e_{3,2}-e_{2,3}=b_2x_2+b_3x_3 \quad in\ \Sigma\\
&e_2n_2+e_3n_3=0 \quad on\ \partial\Sigma
\end{aligned}
\tag{25}
$$

In (24)-(25), Σ and $\partial\Sigma$ are the cross-sectional domain and its boundary, n_α are components of the outward unit normal vectors on $\partial\Sigma$, and coefficients a_α and b_α are linear functions of the strain measures k_α and their s-derivative. Such coefficients, which also depend on the beam's initial shape through the taper coefficients Λ_2 and Λ_3, are given by

$$
\begin{aligned}
a_2&=+2(1+\nu)k_3'+2(1+\nu)\left(\Lambda_3^{-1}\Lambda_3'+2\Lambda_2^{-1}\Lambda_2'\right)k_3\\
a_3&=-2(1+\nu)k_2'-2(1+\nu)\left(\Lambda_2^{-1}\Lambda_2'+2\Lambda_3^{-1}\Lambda_3'\right)k_2\\
b_2&=-2\nu k_2'-2(1+\nu)\Lambda_2^{-1}\Lambda_2'k_2\\
b_3&=-2\nu k_3'-2(1+\nu)\Lambda_3^{-1}\Lambda_3'k_3
\end{aligned}
\tag{26}
$$

The approach used can also provide relations for the components E_{22}, E_{33}, and E_{23} of E, related to the in-plane deformation of the transverse cross-sections, plus the relevant PDEs problem. It is worth noting that the components of the stress resultants (16) depend on the components E_{11}, E_{21}, E_{31} of E, and the additional term $E_{SV}=E_{22}+E_{33}+2\nu E_{11}$, which is related to the aforementioned in-plane deformations. However, we also note that in the present case E_{SV} is of higher order with respect to other terms in the expressions of the stress resultants [18], and vanishes for prismatic beams [4,23]. Hereafter, we do not go into the details of the problem related to the in-plane deformation. Instead, we proceed to study the effects of the cross-sectional taper included in functions e_1, e_2, and e_3, which significantly affects the stress and strain fields in the non-prismatic structures considered in this work.

3.1 The case of the bi-tapered elliptical cross-sections

Let us consider non-prismatic beams with bi-tapered elliptical cross-sections. For such case we can provide analytical closed-form solutions, while for generic cross-sectional shapes the PDEs problems introduced in the foregoing have to be solved with the aid of numerical methods. However, this is not surprising. In fact, analytical solutions are available only for a limited number of cases even in the classical linear theory of prismatic beams [4].

In this case, problems (24)-(25) can be solved without resorting to numerical methods. In particular, we obtain the following analytical results

$$
\begin{aligned}
e_1&=\frac{d_3^2-\rho^{-2}d_2^2}{d_3^2+\rho^{-2}d_2^2}k_1x_2x_3\\
e_2&=+\frac{c_\alpha x_\alpha x_3}{d_3^2\Lambda_3^2}+\frac{c_3+a_2d_2^2\Lambda_2^2}{2}\left(\frac{x_2^2}{d_2^2\Lambda_2^2}+\frac{x_3^2}{d_3^2\Lambda_3^2}-1\right)\\
e_3&=-\frac{c_\alpha x_\alpha x_2}{d_2^2\Lambda_2^2}-\frac{c_2-a_3d_3^2\Lambda_3^2}{2}\left(\frac{x_2^2}{d_2^2\Lambda_2^2}+\frac{x_3^2}{d_3^2\Lambda_3^2}-1\right)
\end{aligned}
\tag{27}
$$

In (27), d_2 and d_3 are the major semi-axes of a reference elliptical cross-section (e.g. the one at the root section), while coefficients c_2 and c_3 are defined as follows

$$c_2 = (b_2 + \rho^2 a_3)(1+3\rho^2)^{-1}\Lambda_3^2 d_3^2$$
$$c_3 = (b_3 - \rho^{-2} a_2)(1+3\rho^{-2})^{-1}\Lambda_2^2 d_2^2 \quad (28)$$

where $\rho=\Lambda_3/\Lambda_2$ is a known function of z_1. Using such results, we can also calculate the strain fields in the structure (23), and the corresponding stress fields. An important result is that the effects of the cross-sectional taper appear explicitly in all above equations in terms of two application-oriented functions, i.e. the taper coefficients Λ_2 and Λ_3. It is also worth noting that the model and results presented so far generalize those of the linear theory of prismatic beams [4,23] and reduce to the them for prismatic beams undergoing small displacements.

Unfortunately, analytical solutions to problems (24)-(25), like those shown here (27), can be obtained only for a few cases. However, such problems can always be solved with the aid of numerical methods for all other cases as well.

4 NUMERICAL EXAMPLES

In this section we show the results obtainable via the modeling approach introduced in the previous sections. The model has been implemented in a numerical code written in the Matlab language, referred to as 3D-BLM. The results from 3D-BLM in terms of displacement, strain and stress fields are compared with those from 3D-FEM simulations performed with Ansys to show the computational efficiency and accuracy of the proposed approach.

In the test case reported here, we consider a straight beam, with bi-tapered elliptical cross-sections, undergoing large displacements. The reference transverse cross-section at the root has its major semi-axes equal to d_2=2m (edgewise) and d_3=2m (flapwise). The dimensions of the other cross-sections reduce from the root to the tip, with linear reduction edgewise (equal to 50% at the tip) and parabolic reduction flapwise (85% at the tip). The material properties are described in terms of reference values of Young's modulus, 70GPa, and Poisson's ratio, 0.25. The structure is fixed at one end (the root), and loaded at the other (the tip) by a flapwise force, F, of progressively increasing magnitude, as shown in Figure 3 (left).

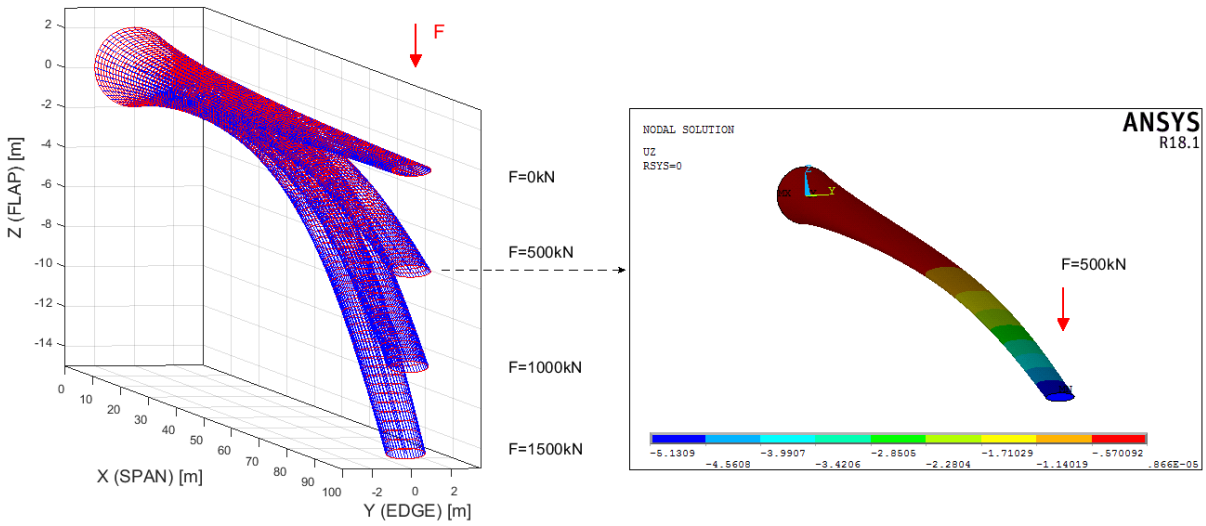

Figure 3: Global deflection with 3D-BLM for increasing F (left) and 3D-FEM for F=500kN (right)

The results obtained from 3D-BLM, and those given by nonlinear 3D-FEM simulations, are now summarized. Specifically, Figure 3 (left) shows the structure's un-deformed shape (F=0), its deformed shapes obtained from 3D-BLM for F=500kN, F=1000kN, F=1500N (left), and the deformed shape given by 3D-FEM for F=500kN (right). Figure 4, instead, presents comparisons in terms of tip-displacements (left) and simulation times (right), which show the computational efficiency and accuracy of the proposed modeling approach.

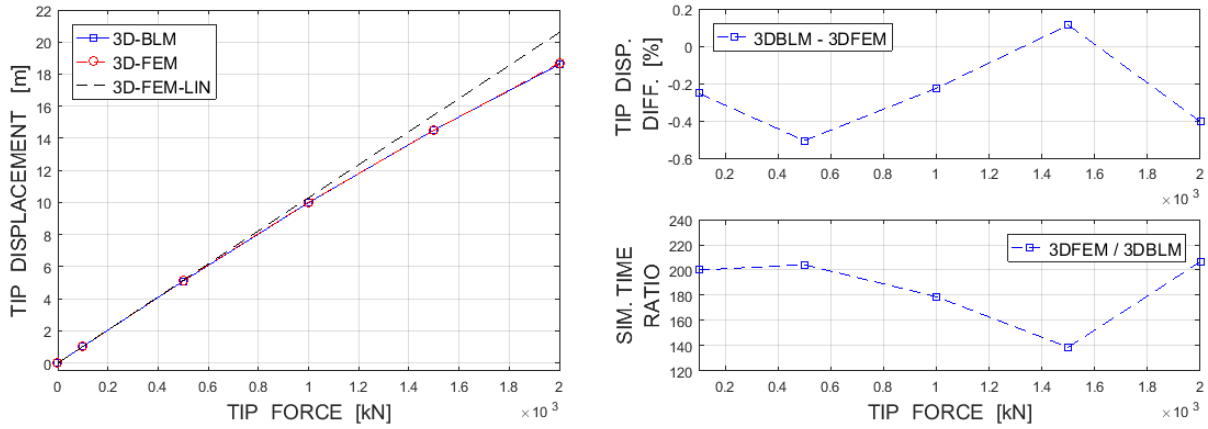

Figure 4: Comparison of tip-displacements (left), tip-displacement differences and simulation times (right)

Apart from such results, the proposed model (3D-BLM) can also provide other meaningful information, such as the rotation of the local triads, the 1D strain measures (8)-(9), the 3D strain fields (13), and the corresponding stress fields (15) and stress resultants (16).

By way of example, in the following we compare the results obtained from 3D-BLM with those obtained from nonlinear 3D-FEM in terms of Cauchy stress fields. Specifically, the comparisons are for the longitudinal normal stresses C_{XX}, in Figure 5, and the transverse shear stresses C_{ZX}, in Figure 6, for a tip-force F=1500kN (which corresponds to a tip-displacement of about 14.2m), at three reference cross-sections (i.e. 30%, 50%, 70% spanwise). In general, we have observed that the normal stresses follow a Navier-like distribution in the transverse cross-sections (they are almost linear in x_3), while the transverse shear stress distributions are quite different from those predictable by the linear theory of prismatic beams. In fact, the shear stresses in non-prismatic beams do not generally vanish at the cross-section's boundary and their distributions can change from cross-section to cross-section (i.e. spanwise).

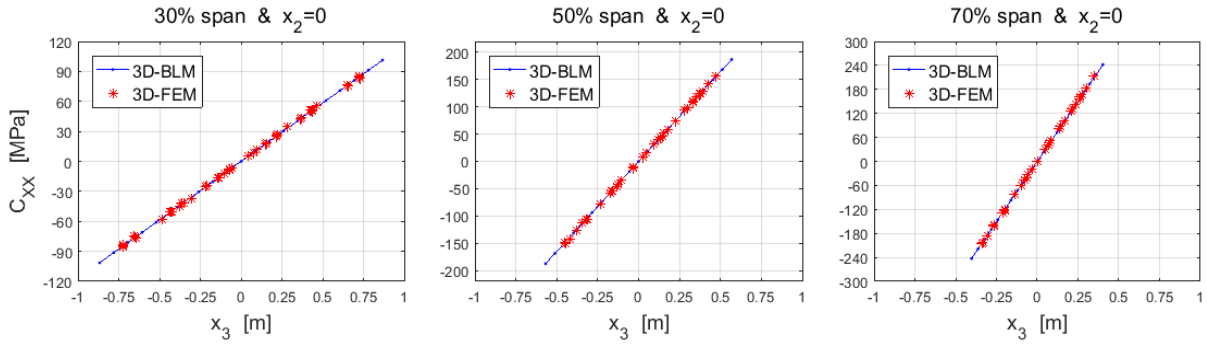

Figure 5: Comparison of longitudinal stress C_{XX} in cross-sections at 30%, 50%, 70% span, for F=1500kN

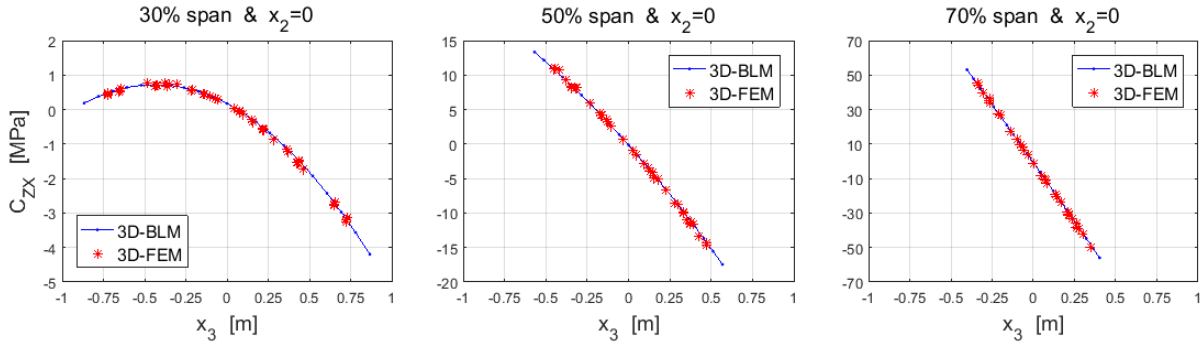

Figure 6: Comparison of transverse shear stress C_{ZX} in cross-sections at 30%, 50%, 70% span, for F=1500kN

Similar results have been obtained for other cross-sections and tip-forces, as well as for other geometries (see, e.g., [18]). In all cases the results obtained confirm the computational efficiency and accuracy of the proposed approach compared to nonlinear 3D-FEM.

The proposed model can thus be used to predict the mechanical behavior of non-prismatic beamlike structures as those considered in this work, which may undergo large displacements of the centre-line's points, warping of the transverse cross-sections in and out of plane, and small strains, as it can furnish accurate information on the deformed states of such structural elements in terms of displacement, strain and stress fields.

6 CONCLUSIONS

Many complex engineering structures, e.g. blades of wind turbines and helicopters, are beamlike and non-prismatic. Their mechanical behavior can be simulated by exploiting 3D beam models which are computationally efficient, accurate, and explicitly consider the main geometric design features of such structures, the large deflections of their centre-line and the 3D warping of their transverse cross-sections. In this work, non-prismatic beamlike structures have been modeled analytically. Their main geometric features (e.g. the cross-sectional taper) have been explicitly included in the model. The approach presented has been shown to be suitable for large deflections of the centre-line and small warping of the cross-sections. The 3D strain tensor has been calculated analytically in terms of the structure's geometric parameters, 1D strain measures and 3D warping fields. A variational approach has been exploited to obtain suitable warping fields. The analytical results obtained for bi-tapered beams, which generalize those of the linear theory of prismatic beams, have been presented and compared to the results of nonlinear 3D-FEM analyses. The results presented confirm the effectiveness of the modeling approach and show the information it can provide.

REFERENCES

[1] Ashwill T.D., Kanaby G., et al, Development of the swept twist adaptive rotor (STAR) blade, 48th AIAA Aerospace sciences meeting, Orlando, FL, Jan. 4-7, 2010.

[2] Bak C., Zahle F., et al., Description of the DTU 10MW reference wind turbine, DTU Wind Energy Report-I-0092, Denmark, 2013.

[3] Wang L., Liu X., Kolios A., State of the art in the aeroelasticity of wind turbine blades: aeroelastic modelling, Renewable and sustainable energy review, 64, 195-210, 2016.

[4] Love A.E.H., A treatise on the mathematical theory of elasticity, 4th ed., Dover

Publications, NY, 1944.
[5] Timoshenko S.P., Goodier J.N., Theory of elasticity, 2nd ed., McGraw-Hill, 1951.
[6] Reissner E., On finite deformation of space curved beams, Journal of applied mathematics and physics, 32, 734-744, 1981.
[7] Hodges D.H., Geometrically exact equations for beams, Encyclopedia of Continuum Mechanics, Springer Verlag, Germany, 2018.
[8] Antman S.S., Warner W.H., Dynamical theory of hyper-elastic rods, Arch. Rational Mech. Anal., 23, 135-162, 1966.
[9] Rubin M.B., Cosserat theories: shells, rods and points, Solid mechanics and its applications, Springer Netherlands, 1st ed., 2000.
[10] Simo J.C., A finite strain beam formulation, the three-dimensional dynamic problem, part I, Computer methods in applied mechanics and engineering, 49, 55-70, 1985.
[11] Berdichevsky V.L., On the energy of an elastic rod, Journal of Applied Mathematics and Mechanics, 45, 518-529, 1981.
[12] Yu W., Hodges D.H., Ho J.C., Variational asymptotic beam-sectional analysis - an updated version, International journal of engineering science, 59, 40-64, 2012.
[13] Ruta G., Pignataro M., Rizzi N., A direct one-dimensional beam model for the flexural-torsional buckling of thin-walled beams, Journal of Mechanics of materials and structures, 1, 1479-1496, 2006.
[14] Kunz D.L., Survey and comparison of engineering beam theories for helicopter rotor blades, J. of Aircraft, 31, 473-479, 1994.
[15] Rafiee M., Nitzsche F., et al., Dynamics, vibration and control of rotating composite beams and blades: a critical review, Thin-walled structures, 119, 795-819, 2017.
[16] Rosen A., Structural and dynamic behavior of pre-twisted rods and beams, American Society of Mechanical Engineers, 44, 483-515, 1991.
[17] Migliaccio G., Ruta G, et al., Curved and twisted beam models for aeroelastic analysis of wind turbine blades in large displacements, XXIV AIMETA conference, 15-19 Sept. 2019, Rome, Italy, Lecture notes in mechanical engineering, Springer, 2020.
[18] Migliaccio G., Ruta G., et al., Beamlike models for the analyses of curved, twisted and tapered horizontal-axis wind turbine (HAWT) blades undergoing large displacements, Wind Energy Science, 5, 685-698, https://doi.org/10.5194/wes-5-685-2020, 2020.
[19] Pai P.F., Three kinematic representations for modeling of high flexible beams and their applications, International Journal of solids and structures, 48, 2764-2777, 2011
[20] Danielson D.A., Hodges D.H., Nonlinear beam kinematics by decomposition of the rotation tensor, Journal of applied mechanics, 54, 258-262, 1987.
[21] Argyris J., An excursion into large rotations, Computer methods in applied mechanics and engineering, 32, 85-155, 1982.
[22] Migliaccio G., and Ruta G., Rotor blades as curved, twisted, and tapered beam-like structures subjected to large deflections, Engineering Structures, 222:111089, 2020.
[23] Gurtin M.E., An introduction to continuum mechanics, Mathematics in science and engineering, Academic Press, 1st ed., 1981.
[24] Courant R., Hilbert D., Methods of mathematical physics, Interscience Publisher, 1st ed., 1953.